Laboratory Models of Bay-Type Continental Shelves in the Winter[1]

TAKASHIGE SUGIMOTO

Ocean Research Institute, University of Tokyo, 1-15-1 Minamidai, Nakanoku, Tokyo, 164, Japan

JOHN A. WHITEHEAD

Department of Physical Oceanography, Woods Hole Oceanographic Institution, Woods Hole, MA 02543

(Manuscript received 3 January 1983, in final form 28 June 1983)

ABSTRACT

A laboratory experiment consisting of a shallow sea of constant depth bounded by a deep ocean through a uniformly sloping continental rise was conducted. The experiment is cooled from above, and there is a region that exhibits sinking convection cells which form the coldest water. This water then spills off the rhs of the shallow sea as a density current (looking downstream for counterclockwise rotation) and forms bottom water in the deep experimental ocean. There are three regimes: for very slow (scaled) rotations there is one big gyre in the shallow sea, and the sinking (convection) region is near the coast; for faster rotations, there are two or three gyres, and for even faster rotations, there are many gyres. In this latter case, the sinking regions are very patchy and sporadic. Comparison with theoretical estimates of temperature difference between the coldest shelf water and the offshore water (based upon the assumption that the density current removes all the cold water) was good but yielded somewhat low predictions.

1. Introduction

If waters in a shallow sea are subjected to high levels of surface cooling and evaporation for a sufficiently long period, it is reasonable to expect them to be denser than water in the neighboring deep ocean. This is due to the effect of surface evaporation and sensible cooling, both acting to decrease temperature and the former acting to increase salinity as well. In many cases this denser water stays confined on the shelf due to the action of wind setup or because of topographic barriers. In other cases, the water is observed to spill off the edge of the shelf and irreversibly contribute in either small or large measure to the deep waters of the world's oceans. An outstanding and important example of this latter class of shelf flow is the flow off the shelf of the Weddell Sea, as discussed by Gill (1973) and Killworth (1979). The recent observation by Foldvik (1979) of a strong bottom current coming off the Weddell Sea through the Filchner depression emphasizes the importance of shelf regions in generating the thermohaline structure of the oceans. Other field areas which have outpouring dense water are the approaches to the Seto Inland Sea in Japan (Endoh, 1983a,b), the shelf in the Gulf of Mexico (Nowlin and Parker, 1974), the Adriatic Sea and big bays of inverse estuary type such as Spencer Gulf in Australia (Bye and Whitehead, 1975).

Flows in a laboratory model of a shelf, cooled from above, will be described here. The primary purpose of the study is to clarify the dynamical processes on the shelf and shelf break which control the exchange of mass and heat between shelf and offshore water. For this first attempt, we confined our interest to the bay-type shelf which has sidewalls on the right and left. (In this paper all references to right or left hand will assume that the reader is looking offshore with the basin rotating counterclockwise.) It is adjacent to a deep "ocean", connected by a shelf break with a steep slope. The deep ocean is exposed to a metal offshore sidewall which is maintained at a constant temperature by a heater connected to a thermostatic bath. The shelf, slope and ocean are all cooled by a top lid which contains chilled water. It differs from models of bays in lakes (Brocard *et al.*, 1977; Brocard and Harlemann, 1980) in that the entire system is rotating. This and the complex bottom configuration differentiate these experiments from models of cooled oceans (Stommel, 1962; Rossby, 1965; Phillips, 1966; Beardsley and Festa, 1972).

The experiments all demonstrated the following flows. First, the fluid rose upward at the heated offshore wall and then flowed toward the shelf, curving toward its right. This plume is somewhat like those studied by Endoh (1983a,b), Harashima and Oonishi (1981) and Beardsley and Hart (1978) who did either nu-

[1] Woods Hole Oceanographic Institution Contribution No. 5336.

merical or hydraulic model experiments dealing with the density current induced by a local heat (or fresh water) supply near the side wall of a closed basin having uniform depth. As this warmed water flowed, it had a mixed (convection) layer with convection rolls aligned in the direction of shear. This water migrated toward the inner coast and became cooler until it reached the temperature of the bottom water. Where this occurred, sinking regions with the densest water in the experiment were formed.

A secondary objective was to observe the nature and fluid dynamics of the sinking (convection) regions on the shelf. The question of the size of sinking regions and their dynamics is fundamental to ocean physics and has been recently renewed due to observations of sinking regions in the Weddell Sea (Gordon, 1978), in the Labrador Sea (Clarke and Gascard, 1979) and in the Mediterranean (MEDOC group, 1970). Some aspects of the dynamics are also discussed by Gill (1973) and Killworth (1979).

The dense water then spreads from its formation region across the shelf and plunges off the shelf break as a gravity current. This current is primarily on the right-hand side wall and appears to be the greatest, but not the exclusive, mechanism for removing the dense water from the shelf. Some effects of rotation on hydraulic control of outflowing dense water at a strait and over a sill has been studied by Stern (1972, 1974), Gill (1976, 1977), Shen (1978), Whitehead, Leetmaa and Knox (1974), Bye and Whitehead (1975), Sambuco and Whitehead (1976), Whitehead and Porter (1977), Rydberg (1980) and Whitehead (1980). One of the objectives of the present experiment is to understand the role of internal Froude number control (critical control) at the shelf break for the outflowing bottom water and possibly for the inflowing water.

Finally, the dense water plunges to the bottom of the ocean and exhibits a hydraulic jump. Little, if anything, is known of the behavior of hydraulic jumps under rotation.

With so many dynamical features occurring at once, the experiment is extremely complicated. We have tried to be as quantitative as possible; however, the qualitative picture of what actually occurs (sketched above and described in more detail in Section 3) may also be of benefit.

2. Scaling considerations

The basic processes of the phenomena are the basin-scale shelf circulation, the cascading flow of shelf bottom water across the shelf break and small-scale convection in the upper layer. Let us start with the steady Boussinesq approximations to the continuity, momentum and heat equations

$$\nabla \cdot \mathbf{u} = 0, \tag{2.1}$$

$$(\mathbf{u}\cdot\nabla)\mathbf{u} + f\mathbf{k}\times\mathbf{u} = -\frac{1}{\rho_0}\nabla p + \nu\nabla^2\mathbf{u} - g\alpha T\mathbf{k}, \tag{2.2}$$

$$(\mathbf{u}\cdot\nabla)T = \kappa\nabla^2 T, \tag{2.3}$$

where $\mathbf{u}$ is cartesian velocity vector, ρ_0 is the mean density of the water, p is pressure, f the Coriolis parameter, ν is viscosity, g the gravitational acceleration, α the coefficient of thermal expansion, T is temperature anomaly around the mean value, κ is thermal diffusivity and $\mathbf{k}$ is a unit vector in the vertical direction. The external variables are heat flux H (as will be explained in the experimental section), angular rate of rotation Ω or $f/2$, and geometry of the experiment which at this point is depth d and width L of the shelf region. For scaling purposes it will be assumed that volumetric flux off the edge of the shelf obeys the rotating hydraulics relation

$$Q = \frac{1}{2}\frac{g\alpha\Delta T d^2}{f}, \tag{2.4}$$

where ΔT is the temperature difference between the deep ocean water (which is close to the temperature of the fluid coming into the shelf in the top mixed layer) and the shelf water (which is close to the temperature of the coldest water). The above assumption will be valid if there is a density current on the right-hand wall, if the current is as deep as the shelf (which will maximize mass flux off the shelf), and if there is a geostrophic balance across the current. We presume that this current removes most of the cooled water from the shelf. In that case, heat flux H off the shelf is

$$H = \rho C_p Q\Delta T = \frac{\rho}{2f} C_p g\alpha\Delta T^2 d^2, \tag{2.5}$$

where C_p is specific heat. Since H and f are externally controlled variables in the experiment and all the rest of the variables in 2.5 are properties of the fluid except for ΔT, 2.5 defines a temperature scale

$$\Delta T = \left(\frac{2fH}{\rho C_p g\alpha d^2}\right)^{1/2}. \tag{2.6}$$

Next, the horizontal velocity scale will be taken to be the velocity of a geostrophic density current of height d and width L, where

$$U = \frac{g\alpha\Delta T d}{2fL}$$

which, using (2.6), leads to a horizontal velocity scale of

$$U = \left(\frac{g\alpha H}{2\rho C_p f L^2}\right)^{1/2}. \tag{2.7}$$

For the moment we will use as the vertical velocity scale w, the results of the continuity equation with the preceding scaling parameters (i.e. $w = (g\alpha H/2\rho C_p d^2)^{1/2}$ not-

ing with caution that sinking will not really occur everywhere on the shelf, nor will lateral currents necessarily occupy the entire width of the shelf. The scaled equation (2.2) is therefore

$$D_1(\mathbf{u}\cdot\nabla\mathbf{u}) + \mathbf{k}\times\mathbf{u} = -\nabla p + E\epsilon^2\nabla_H^2\mathbf{u} + E\mathbf{u}_{zz} + 2\epsilon^{-1}T\mathbf{k},$$

where

$$\left.\begin{aligned}\epsilon &= \frac{d}{L}\\ E &= \frac{\nu}{fd^2}\\ D_1 &= \left(\frac{g\alpha H}{2\rho C_p f^3 L^4}\right)^{1/2}\end{aligned}\right\}. \tag{2.8}$$

The last dimensionless number is the ratio of inertia to Coriolis forces and thus is a Rossby number of the form $(g\alpha\Delta Td/2f^2L^2)$ [using (2.5)] or U/fL [using (2.6)].

The energy equation (2.3) is

$$D_2(\mathbf{u}\cdot\nabla)T = \epsilon^2\nabla_H^2 T + T_{zz},$$

where

$$D_2 = \left(\frac{g\alpha H}{2\rho C_p f\kappa^2}\right)^{1/2}\epsilon^2 \tag{2.9}$$

is the ratio of lateral advection by a density current to vertical diffusion and is equal to D_1/EP_r, where Pr is Prandtl number ν/κ. In our experiment we want to make E small and D_2 large so that advection rather than diffusion dominates the heat and momentum transfer in the interior of the fluid. We also will let D_1, hence the Rossby number, be varied as widely as possible.

3. Model and experimental facilities

a. The apparatus

The main part of the experimental apparatus is a rotating, rectangular basin which consists of a square shelf (50 cm × 50 cm × 5 cm deep) connected by a narrow (10 cm wide) slope to a deeper basin (30 cm × 50 cm × 15 cm deep) mounted on a turntable as is shown in Fig. 1. The enclosed fluid is cooled through a top lid and is also heated through the offshore side wall which is made of a painted aluminum plate. The outside of this plate is in contact with a stirred heated bath. Temperature of the hot bath is maintained by 500 W thermostated heaters. The temperature fluctuations of the cold bath and the hot bath are less than ±0.05°C and approximately ±0.1°C, respectively. The top plate was made from Plexiglas plate. The lid is designed to be cooled with water as follows: the bottom of the lid is composed of Plexiglas plate 6 mm (¼ inch) thick. Above this is a channel

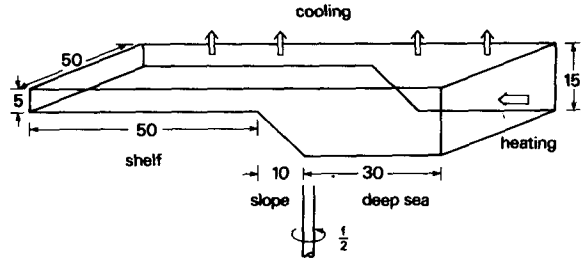

FIG. 1. Perspective sketch of the experimental apparatus.

6 mm deep, 56 cm wide and 91 cm long, through which chilled water is made to flow. The channel is covered above by a second 6 mm Plexiglas plate. Running water is introduced at one end of the lid and removed at the other end. This water comes from a bath which is cooled by refrigeration, and temperature regulated by a thermostat. Pipes between the cooler and cold bath were insulated and connected to the turntable via a swivel connector to get cold water onto the turntable. Temperature difference between the test fluid and the water in the upper lid was much greater than that in the model fluid, so to a first approximation, the fluid was cooled uniformly from above according to the formula

$$H = kA\Delta T_p/\delta, \tag{3.1}$$

where k is conductivity of the Plexiglas (5×10^{-4} cal $s^{-1}\,°C^{-1}\,cm^{-1}$), A area of the lid over the test section (2500 cm^2), ΔT_p temperature difference between chilled water and the test fluid and δ is thickness of the plate (6 mm). Thus, the cooling rate of the water on the shelf (2500 cm^2) from above is

$$H = 2.08\Delta T_p \text{ calories per second}, \tag{3.2}$$

which at steady state equals the heat inflow from the deep basin. The side walls and the bottom of the test chamber were made of Plexiglas plate, 12.6 mm in thickness for better insulation. The main basin was placed in a rectangular plate glass tank which was 59.5 cm × 111.5 cm × 21 cm deep (inside dimensions), and the top cold bath was fixed with screws to the main basin. Sidewall heat loss was less than one percent of the heat flux in the experiment due to thicker sidewalls and an average experimental temperature close to room temperature.

b. Measurement technique

Photographs of the current pattern were taken by 35 mm camera and a 16 mm movie camera located above the basin. For visualization of the flow, the test fluid was buffered to be close to the transition pH for the pH-sensitive indicator thymol blue (Merzkirch, 1974). A voltage was applied between wires of 0.01 mm in diameter which were stretched at 1 and 4 cm depths in the test fluid. This resulted in the fluid near

the wires changing from a yellow color to a dark blue. It was possible to trace the movement of this fluid for a number of minutes thereafter. Temperature in the basin was measured by a thermistor put on a thin glass tube of 3 mm diameter. Time constant of the thermistor is 0.25 s. It was moved vertically by the use of an electric motor at a speed of 0.5 mm s^{-1}. By this means, a continuous vertical profile of temperature was recorded by a pen recorder. Data were taken at a number of "stations" through small holes in the lid. The temperature data above the temperature maximum in the convecting layer was discarded because rising traverses gave different temperatures from descending traverses in that region.

c. *Experimental procedure*

The experiment was performed in a laboratory where air temperature was kept at 20.0°C ± 0.5°C. First, water in the hot bath was warmed up to approximately 27°C (a temperature which was higher than maximum temperature of the basin water in the steady state) to de-gas the test fluid, while water was cooled in the cooled thermostatic bath but not circulated in the lid. Then the main basin was started, after which water from the cold bath was started, care was taken not to introduce bubbles both in the main basin and in the top lid.

Then the rotation of the tank was started, and after sufficient time the temperature distribution of the test fluid became steady. It took more than three hours for this to occur. Vertical profiles of the temperature at the stations (shown in the figures in the next section) and the temperature in the hot and cold baths were measured using a thermistor and checked with a thermometer (with accuracy better than ±0.1°C), respectively. Pictures of the current patterns were also taken. The entire measurement procedure took another three hours.

4. Experimental results

a. *Circulation patterns*

Fig. 2 shows dependence of the circulation patterns on the Coriolis parameter (ordinate) and temperature difference between water in hot and cold baths ΔT_e, which is roughly proportional to the heat flux. Dots show the parameters at which experiments were done. Numbers given next to the points signify the number of estimated eddies on the shelf region, and curves separate regions with approximately the same circulation patterns. Although the current patterns change rather continuously, they can be classified into four groups. Qualitative structure of the flows appeared to be governed by the Rossby radius as defined in (2.8). This aspect will be discussed quantitatively in Section 5, but for present purposes, it is sufficient to note that baroclinic flows often develop eddies with a Rossby radius.

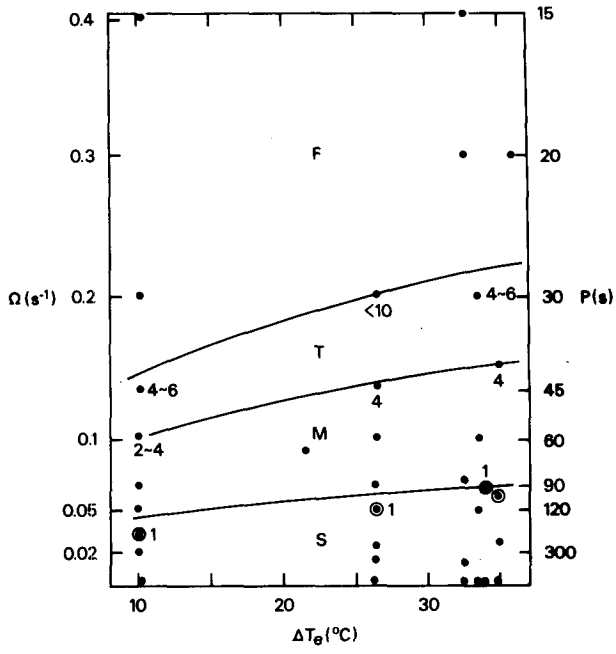

FIG. 2. Location of the experimental parameters in the space of externally controlled variable rotation Ω (=2π/period, p) and external temperature difference ΔT_e. Also delineated are boundaries between the slow (S), moderate (M), transition (T) and fast (F) rotation limits.

1) CASES WITHOUT ROTATION AND SLOW ROTATION—ROSSBY RADIUS IS BIGGER THAN A QUARTER OF THE SHELF (FIG. 3, PLATE 1)

In these cases, vertical circulations are predominant (flow is like a Hadley cell). It is observed that the sinking region is limited to a narrow, inner coastal zone region. The width of the zone is less than two centimeters. On the other hand, the thickness of the thermal plume along the offshore side wall is of the order of a few millimeters. In cases with slight rotation, warm surface water flows toward the inner coastal zone laterally and uniformly. However, cold bottom water from the inner shelf twists slightly to the rhs as shown in Fig. 3c, d.

2) CASES OF MODERATE ROTATION—ROSSBY RADIUS IS OF THE ORDER OF HALF THE SHELF SIZE (FIG. 4, PLATE 2)

Horizontal single gyres of basin-scale are formed on the shelf. Upper flow is cyclonic and lower outflow from the center of the gyre is anticyclonic. Upper inflow from the deeper basin is twisted toward the left, and flow into the inner shelf region is along the left sidewall. On the other hand, lower cold water flows along the shelf break towards the rhs sidewall, hits the wall and goes out from the shelf in a strong downwelling jet on the slope. Width of the jet decreases as the rotation rate is increased. The sinking region is usually on the inner part of the rhs coast

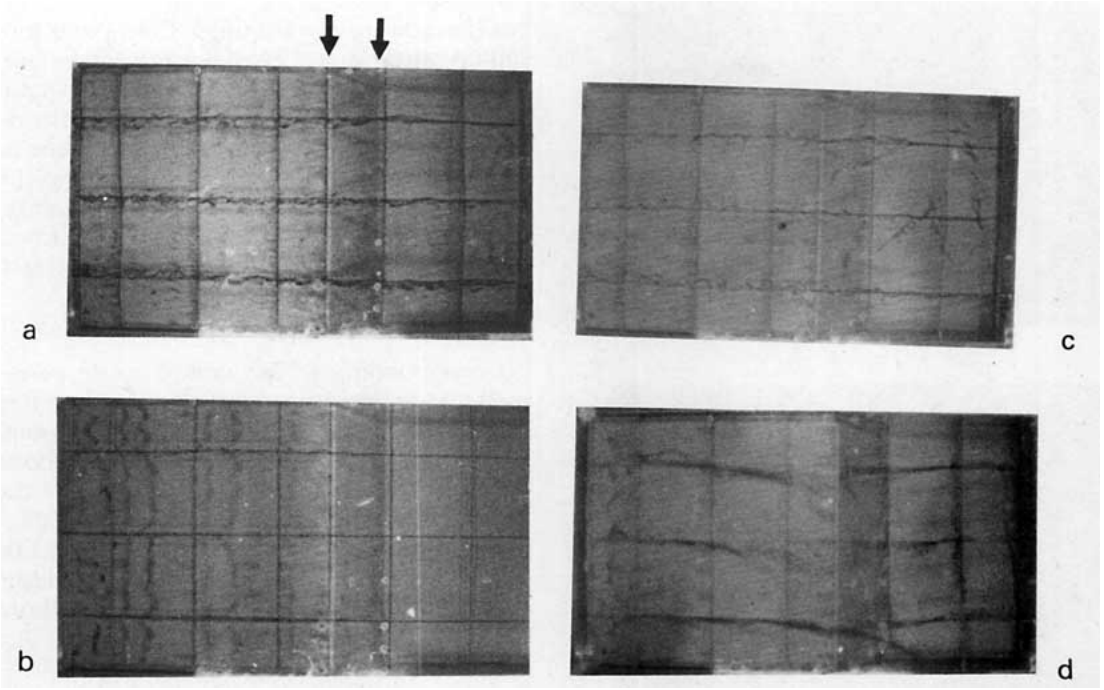

FIG. 3. The experiment as viewed from above with heated sidewall to the right. The edge of the shelf and the bottom of the break are indicated by two arrows, respectively. The voltage feeding the indicator wires was turned on ~30 s before the photographs were taken in a, b and d, and was pulsed in c. Upper layer is (a, c), and lower layer (b, d). For (a, b) $\Omega = 0$, and the flow is strictly like a Hadley cell. For (c, d) $\Omega = 0.015\ s^{-1}$ ($D_1 = 1230 \times 10^{-4}$), and the flow in the lower layer (d) swerves slightly to the right as it flows toward the break. Less swerving is visible in the upper layer (c). These are runs number 10 and 11 in Table 1.

and is turbulent due to small-scale sinking convection cells (Fig. 4c, d). The bottom flow away from the sinking region is laminar. As the rotation rate is increased, curvature of the gyre increases and the gyre tends to retreat toward the inner coastal part of the shelf.

3) TRANSITION FROM MODERATE TO FAST ROTATION—ROSSBY RADIUS IS OF THE ORDER OF BUT SMALLER THAN HALF THE SHELF SIZE (FIG. 5, PLATE 3)

As the rotation rate is increased and the diameter of the gyre is decreased into less than one-quarter of the shelf size, two or more gyres are formed. In the upper layer there are many cyclonic eddies on the whole shelf and also in the offshore region. Most of the strong cyclonic swirl on the shelf penetrates into the bottom layer. Sinking regions now are found to move around and occur in many of the gyres.

4) FAST ROTATION—ROSSBY RADIUS IS MUCH SMALLER THAN HALF THE SHELF SIZE (FIG. 6, PLATE 4)

In this case, turbulent eddies are predominant and fill the shelf as well as the offshore region. They are mostly cyclonic in the upper layer and anticyclonic in the lower layer but in some cases are less baroclinic than those in Case 3. Occasionally a gyre is cyclonic from top to bottom. The size of the eddies is decreased as the rotation rate is increased. On the average, the shelf bottom water flows slowly along the shelf break toward the right-hand side wall and flushes out as a downwelling jet at the right-hand wall. Cyclonic eddies on the shelf break also contribute to the flushing of the shelf water. Warm surface water from offshore enters into the shelf intermittently in the upper layer above the shelf break as well as along the left-hand side wall.

b. Thermal structures

Vertical sections in the longitudinal direction (17.5 cm from the right side wall) from the inner coast of the shelf to the offshore side wall and lateral sections at the shelf break of the temperature were drawn. Temperature difference between the waters in the hot and cold baths ΔT_e was kept at 26.4°C. Thermal structures corresponding to the previous four groups of current patterns are as follows.

1) CASES WITHOUT ROTATION AND SLOW ROTATION (FIG. 7)

In both figures we see thermal effluents of about 2.5 cm thick extend from the offshore side wall towards the shelf. They are cooled down fairly rapidly but intrude close to the coast. Regions which are probably well-mixed in the vertical, sometimes exhibited small-scale fluctuations due to convection cells. Regions where there was clear evidence of con-

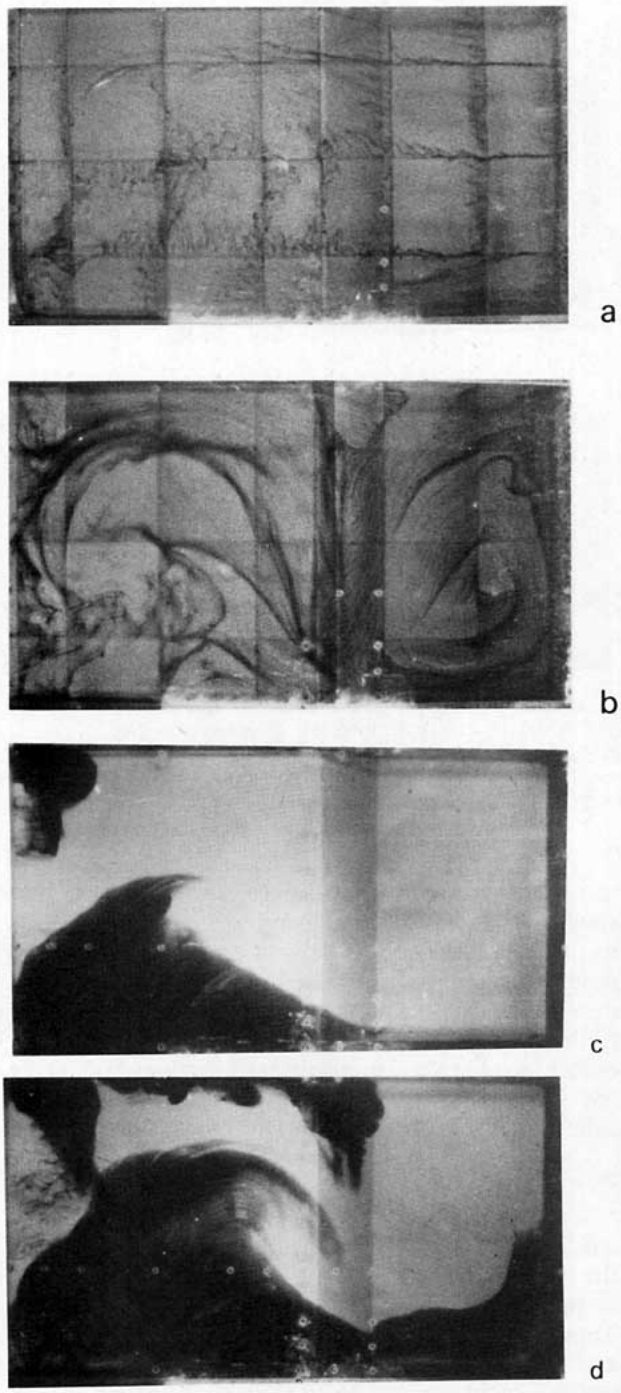

FIG. 4. Moderate rotation. One large eddy on the shelf: (a) upper layer and (b) lower layer. The rotation is $\Omega = 0.52\ s^{-1}$ and $D_1 = 190 \times 10^{-4}$; this is run number 12 in Table 1. In (c) and (d) (with slightly different parameters), the color of the dye was changed by injecting a very dilute solution of NaOH. The slightly clear patches in the lower left are the convection cells. The fine streaks in the dye occur in the bottom Ekman layer; (d) is two minutes later than (c).

vection cells lie above the dashed line. These cells were usually roll cells aligned in the direction of flow of the top mixed layer. Upper layers were well mixed, but lower layers are stratified. Cold water formed by sinking at the inner coastal zone comes out in the bottom of the lower layer and falls down along the slope. Fig. 8 (Plate 5) is a photograph of the side view of the shelf break in the case without rotation in which we see a stationary bore of ~5 cm in height at the foot of the slope. When there is slight rotation, this cascading flow is turned conspicuously towards the right and the width becomes thinner downstream.

2) CASES OF MODERATE ROTATION (FIG. 9)

Corresponding to the typical single gyre on the shelf, the temperature fields show cold domes in the central region and a thermal front at the shelf break. For a little faster rotation rate, the cold domes and the front retreat toward the inner part of the shelf. Warm offshore water comes into the shelf along both the right-hand and left-hand side walls and then circulates cyclonically on the shelf. The width of the front associated with inflow and outflow through the shelf break is reduced as the rotation rate is increased, as is shown in the lateral section at the shelf break. The density fields are stratified on the average, except at some spots where there are a few convection cells penetrating to the lower layer in the central regions, and the inner left-hand side corner. Cold bottom water made by the sinking (and swirling) cells comes

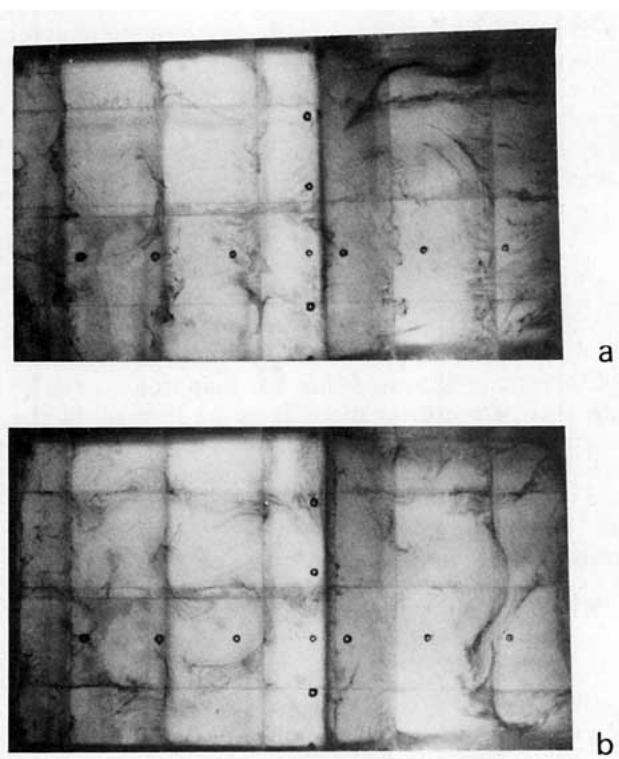

FIG. 5. Transition from moderate to fast rotation. As before (a) upper layer and (b) lower. Parameters are $\Omega = 0.210\ s^{-1}$ and $D_1 = 24 \times 10^{-4}$l (run 14).

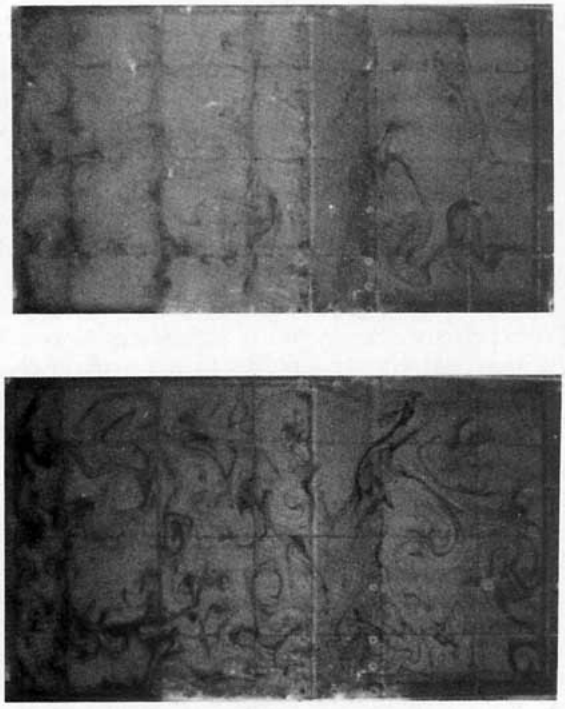

FIG. 6. Fast rotation with many eddies, $\Omega = 0.419$, $D_1 = 8 \times 10^{-4}$ (run 15).

out from the inner coastal region, generating anticyclonic circulation. A strong jet in the lower layer flows along the shelf break toward the right-hand side in the lower layer, hits the right wall and cascades down the slope along the right wall.

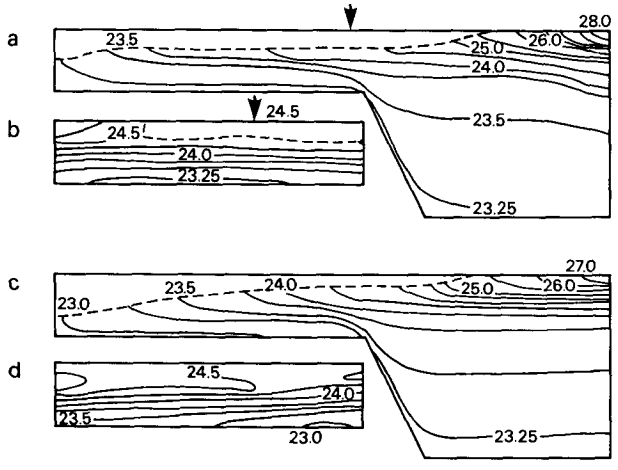

FIG. 7. Temperature sections from coast to offshore sidewall (a, c) and across the shelf break (b, d) for zero (a, b) and very slow (c, d) rotation. The location of sections (a, b) are shown by arrows in (b, a). The cross shelf section is looking offshore. Above dashed lines are convection regions and temperatures were variable and sometimes with small scales. Isotherms are drawn every 0.25°C interval below 25°C and every 0.5°C above. Parameters correspond to those in Fig. 3.

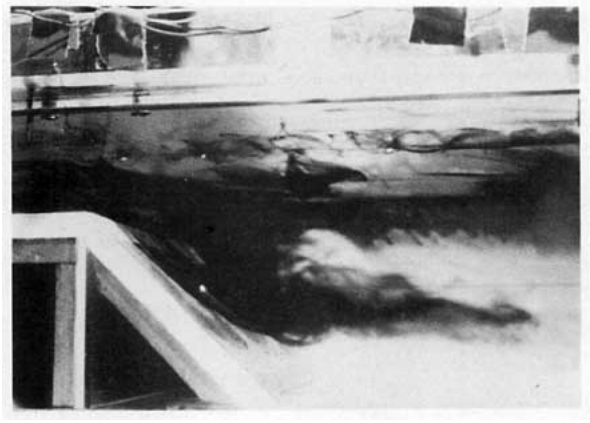

FIG. 8. Side view of a hydraulic jump near the bottom of the shelf break next to the right-hand wall. Convection rolls are also visible near the top lid of the apparatus.

3) MODERATE AND FAST ROTATION RATES (FIG. 10)

Temperature varies significantly at each spot due to turbulent eddies, and each vertical profile thereby differs. However, these figures still show macroscopic thermal structures and, in particular, a distinct thermal front is formed at the shelf break again, although the front wanders around and varies in association with turbulent eddies.

5. Dynamical control of mass and heat exchange between shelf water and offshore water

It is useful to understand how the density current and water exchange is controlled at the shelf break and also how the temperature difference between the shelf water and offshore water depends on externally controlled parameters such as heating–cooling rate and rotation rate of the model.

Eq. (2.4) for the mass flux, i.e., $Q = g\alpha\Delta T d^2/2f$ may be anticipated if the internal Rossby radius is smaller than the width of the shelf, i.e., $D_1 < 1$ [cf., (2.8)]. Using Eq. (2.5) for the heat flux due to a density current cooling the shelf, (3.2) for the heat flux imposed from above, the empirical relation of $\Delta T_p = 0.48\Delta T_e$ in this experiment and the values $g = 980$ cm^2 s^{-1}, α

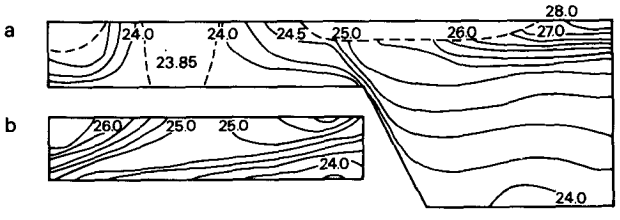

FIG. 9. Sections for moderate rotation, same parameters as Figs. 4a, b. Note the typical doming in the center of the shelf which is actually close to the region of convective sinking. Note also the front at shelf break, and the edge current of warm water at the left-hand coast.

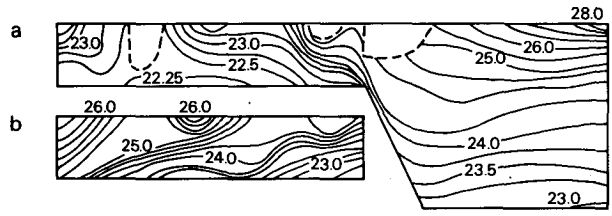

FIG. 10. Section for fast rotation. The "mixed" or sinking regions are considerably more localized and transient. The shelf front and warm coastal current persist.

$= 2 \times 10^{-4}\,°C^{-1}$, $\rho C_p = 1.0$ cal cm^{-3} °C^{-1} and $d = 5$ cm, we obtain a prediction for the temperature jump across the shelf of

$$\Delta T = 0.92(f\Delta T_p)^{1/2} = 0.90(\Omega\Delta T_e)^{1/2}. \quad (5.1)$$

The relevant numbers for the experimental runs are given in Table 1, column 8 and the measured temperature change from the warmest offshore water to the coldest shelf water at mid-depth is given in column 11. A comparison of data in columns 8 and 11 is made in Fig. 11. In this figure, temperature differences are shown between the warmest offshore water and the coldest shelf water at 2.5 cm depth (ΔT^X). Values of the rotation period are given next to the points. Formula (5.1) is shown by a 45° line. Proportionality of the observed temperature difference to the theoretically estimated one is good at fast and moderate rotation rates, although the observed temperature differences are underestimated by a constant factor less than 2.

This difference is not really too surprising in view of the many assumptions made in the theory. Surely the geostrophic balance across the existing dense current is modified by centrifugal forces to some extent, and there must be an offshore flux in the Ekman layer (this has been observed, see Section 7). It would have been very surprising to have had the prediction of temperature difference *smaller* than the observation, since we have underestimated the total offshore flux and overestimated temperature differences as equal to the most extreme differences in the experiment. In fact, the problem could have been cast as a series of statements of plausible inequalities, leading to a safer statement than (5.1), i.e.,

$$\Delta T > 0.90(\Omega\Delta T_e)^{1/2}.$$

It is expected that the radius of the curvature of the circulations on the shelf is roughly proportional to the internal Rossby radius of deformation R_d defined by $R_d = Nd/f$ where d is the depth of the shelf, f the Coriolis parameter and $N = (g\alpha\partial T/\partial z)^{1/2}$ is the Brunt–Väisälä frequency. Using $(\alpha\partial T/\partial z) = \alpha\Delta T^Z/d$ (ΔT^Z is the temperature difference from top to bottom), $N = (g\alpha\Delta T^Z/d)^{1/2}$, $R_d = (g\alpha\Delta T^Z d/f^2)^{1/2}$ and an empirical result that $\Delta T^Z = \Delta T$ (see Table 1 for a comparison), then (5.1) gives

$$R_d = 0.95\,(\Delta T_p/f^3)^{1/4} = 0.47\,(\Delta T_e/\Omega^3)^{1/4}. \quad (5.2)$$

TABLE 1. Experimental measurements and predictions. Column headings are as follows: 2. Hot and cold bath temperature difference, 3. Rotation period, 4. Angular rate of rotation, 5. Rossby number Eq. (2.8), 6. Ekman number ν/fd^2, 7. Ratio of lateral advection to vertical diffusion Eq. (2.9), 8. ΔT Eq. (5.1), 9. R_d Eq. (5.2), 10. Radius of experimental gyre or gyres, 11. Temperature difference between shelf and offshore water, 12. Temperature difference between inflow and outflow waters at the shelf break, 13. Vertical temperature difference on the shelf, 14. Rossby radius Eq. (5.3) based upon observed temperature difference in column 11.

1	2	3	4	5	6	7	8	9	10	11	12	13	14
Run No.	ΔT_e (°C)	p (s)	Ω (s^{-1})	D_1 ($\times 10^{-4}$)	E ($\times 10^{-4}$)	D_2	ΔT (°C)	R_d (cm)	r (cm)	ΔT^X (°C)	ΔT^Y (°C)	ΔT^Z (°C)	R
1	10.0	∞	0.000							0.6			
2	10.0	305	0.021	460	95	48.4	0.41	14.4	33	0.85			21.7
3	10.0	180	0.035	214	57	37.5	0.53	9.8	20				
4	10.0	120	0.052	117	38	30.6	0.65	7.3	16	1.2			10.4
5	10.0	90	0.070	76	28	26.6	0.76	5.8	13	1.4			8.4
6	10.0	60	0.105	41	19	21.6	0.93	4.3	8	1.5			5.8
7	10.0	45	0.140	27	14	18.9	1.07	3.5	7.5	1.6			4.5
8	10.0	30	0.210	15	10	15.3	1.31	2.6	5.5	2.3			3.6
9	10.0	15	0.419	5	5	10.8	1.85	1.5	2.5	2.7			2.0
10	26.4	∞	0.000							1.1	1.0	1.0	
11	26.4	415	0.015	1230	132	93.2	0.57	23.5	54	1.3	1.3	1.3	37.6
12	26.4	120	0.052	190	38	49.7	1.06	9.2	19	2.0	2.0	1.5	13.5
13	26.4	90	0.070	119	28	42.5	1.24	7.3	17.5	2.0	2.2	1.8	10.0
14	26.4	30	0.210	24	10	25.3	2.13	3.3	7.5	3.3	3.5	2.0	4.3
15	26.4	15	0.419	8	5	17.5	3.00	1.9	5	5.0	4.8	3.3	2.6
16	32.5	∞	0.000							1.0			
17	32.5	450	0.014	1523	142	107.3	0.61	26.2	51	1.3			40.3
18	32.5	85	0.074	125	27	46.3	1.40	7.5	14.5	2.0			9.5
19	32.5	15	0.419	9	5	19.4	3.33	2.0	3.5	5.1			2.7

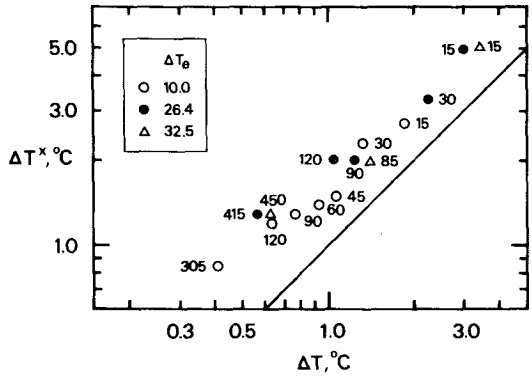

FIG. 11. Relation between the temperature difference between the shelf and offshore ΔT^x and theoretical prediction ΔT with Eq. (5.1). The correlation coefficient is 0.86, but there is a systematic offset.

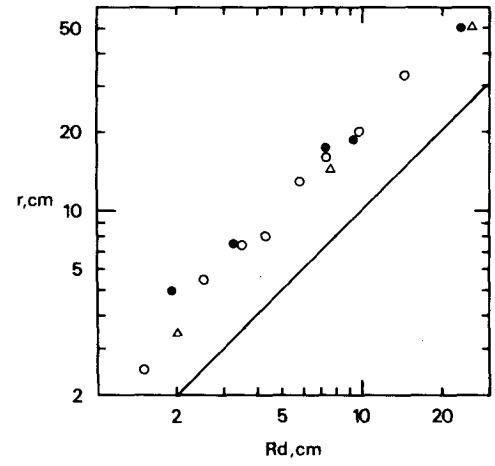

FIG. 12. Relation between radius of curvature r of the eddy or eddies on the shelf and the externally predicted Rossby radius R_d [Eq. (5.2)].

In Table 1 are shown the values of estimated R_d as well as the maximum values of the vertical temperature differences ΔT^Z (column 13) in the frontal region (see Figs. 8–10). Also given is temperature difference between the inflow and outflow waters at the shelf break ΔT^Y (column 12). The longitudinal temperature difference between the shelf water and offshore water at mid-depth ΔT^X, and the other temperature differences (ΔT^Y and ΔT^Z) are all roughly the same size.

Figure 12 shows the dependence of the radius of the curvature of the bottom circulation on the internal Rossby radius of deformation. The radius of curvature of the circulations was determined from photographs by finding best fit arcs. The observations lie above the 45° line of perfect correlation by a little more than a factor of 2. This can be partially attributed to the fact that (5.1) overestimated the temperature difference by approximately a factor of 2. If the observed temperatures ΔT^X from column 11 are used to estimate a Rossby radius from the formula

$$R = \left[\frac{g\alpha\Delta T^X d}{f^2}\right]^{1/2} = \frac{0.4949}{\Omega}(\Delta T^X)^{1/2} \quad (5.3)$$

(using the same values for g, α and d as before), the observed eddy size r agrees more closely with R (Fig. 13), but is still approximately $1.5 \times R$.

6. Concluding remarks

The agreement of experiment and prediction appears to be reasonable given the crude nature of the arguments leading to the prediction. There is one or more gyre on the shelf, generally somewhat bigger than a Rossby radius size, which has one or more patches of sinking fluid. The fluid is removed by a type of geostrophic current at the shelf break near the right-hand wall and it is possible to calculate approximately the magnitude of this current.

There are a number of regions with special processes in this experiment which may exist on real shelves. Along the shelf break there can almost always be found a jet-like front whose nature warrants a separate investigation. The density current on the right-hand wall, and its sizeable mass flux offshore tell us that such currents may occur in oceanic bays, an idea yet to be tested. The nature of the sinking regions tells us that we should search for these in real bays and shallow seas. If parameters are appropriate for the weak rotation limit, we would expect them close to the coast and confined to one or two patches—as they were in this experiment. With parameters characteristic of faster rotation, there would be many patches with fewer cells meandering around like atmospheric squalls. Frontal structure would sometimes be encountered. A more precise view will require more focused experiments.

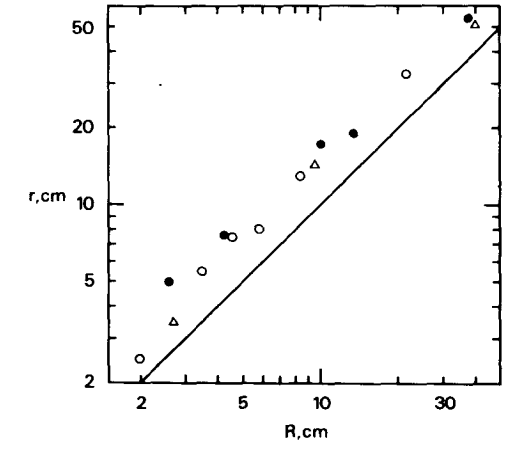

FIG. 13. Relation between radius of curvature r of the eddy or eddies on the shelf and the Rossby radius R based upon observed temperature between shelf and offshore [Eq. (5.3)].

Acknowledgments. Support for T. Sugimoto's visit to the United States was provided by the Ministry of Education, Science and Culture in Japan. Support for the laboratory equipment and the technical assistance of Robert Frazel, who provided valuable laboratory assistance, was provided by the Ocean Sciences Division, National Science Foundation under Grant OCE 78-18322.

REFERENCES

Beardsley, R. C., and J. F. Festa, 1972: A numerical model of convection driven by surface stress and non-uniform horizontal heating. *J. Phys. Oceanogr.*, **2**, 444–455.

——, and J. Hart, 1978: A simple theoretical model for the flow of an estuary onto a continental shelf. *J. Geophys. Res.*, **83**, 873–883.

Brocard, D. N., and D. R. F. Harlemann, 1980: Two-layer model for shallow horizontal convective circulation. *J. Fluid Mech.*, **100**, 129–146.

——, G. H. Jirka and D. R. F. Harlemann, 1977: A model for convective circulation in side arms of cooling lakes. Ralph M. Parsons Laboratory for Water Resources and Hydrodynamics, Tech Rep 223, Dept. Civil Engineering, Massachusetts Institute of Technology.

Bye, J. A. T., and J. A. Whitehead, Jr., 1975: A theoretical model of the flow in the mouth of Spencer Gulf, South Australia, *Estuarine Coastal Mar. Sci.*, **3**, 477–481.

Clarke, R. A., and J. C. Gascard, 1979: Deep convection and the formation of Labrador Sea Water (Abstract). Int. Assoc. Phys. Sci. Ocean (IAPSO) Meeting, Canberra, 369 pp.

Endoh, M. 1983a: Three-dimensional structures of gravity currents in a rotating basin. Part I: A local discharge of buoyancy. *J. Oceanogr. Soc. Jpn*, (in press).

——, 1983b: Three-dimensional structures of gravity currents in a rotating basin. Part II: A thermohaline front in a rotating channel. *J. Oceanogr. Soc. Jpn*, (in press).

Foldvik, A., 1979: Current and tidal measurements in the Weddell Sea (Abstract). Int. Union Geod. and Geophys. 17th General Assembly, Canberra, 421 pp.

Gill, A. E., 1973: Circulation and bottom water production in the Weddell Sea. *Deep-Sea Res.*, **20**, 111–140.

——, 1976: Adjustment under gravity in a rotating channel. *J. Fluid Mech.*, **77**, 603–621.

——, 1977: The hydraulics of rotating channel flow. *J. Fluid Mech.*, **80**, 641–671.

Gordon, A. L., 1978: Deep antarctic convection west of Maud Rise. *J. Phys. Oceanogr.*, **8**, 600–626.

Harashima, A., and Y. Oonishi, 1981: The Coriolis effect against frontogenesis in a steady buoyancy-driven circulation. *J. Oceanogr. Soc. Jpn*, **37**, 49–59.

Killworth, P. D., 1979: On chimney formation in the ocean. *J. Phys. Oceanogr.*, **9**, 531–554.

MEDOC Group—H. Lacombe, P. Tchernia, M. Ribet, J. Bonnot, R. Frassetto, J. C. Swallow, A. R. Miller and H. Stommel, 1970: Observation of formation of deep water in the Mediterranean Sea. *Nature*, **227**, 1037–1040.

Merzkirch, W., 1974: *Flow Visualization.* Academic Press, 250 pp.

Nowlin, W, D., Jr., and C. A. Parker, 1974: Effects of cold-air outbreak on shelf waters of the Gulf of Mexico. *J. Phys. Oceanogr.*, **4**, 467–486.

Phillips, O. M., 1966: On turbulent convection currents and the circulation of the Red Sea. *Deep-Sea Res.*, **13**, 1149–1160.

Rossby, H. T., 1965: On thermal convection driven by non-uniform heating from below: an experimental study. *Deep-Sea Res.*, **12**, 9–16.

Rydberg, L., 1980: Rotating hydraulics in deep-water channel flow. *Tellus*, **32**, 77–89.

Sambuco, E., and J. A. Whitehead, Jr., 1976: Hydraulic control by a wide weir in a rotating fluid. *J. Fluid Mech.*, **73**, 521–528.

Shen, C. 1978: Rotating hydraulics of steady flows in an open channel. *J. Fluid Mech.* **112**, 161–188.

Stern, M. E., 1972: Hydraulically critical rotating flow. *Phys. Fluids*, **15**, 2063–2064.

——, 1974: Comment on rotating hydraulics. *Geophys. Fluid Dyn.*, **6**, 127–130.

Stommel, H., 1962: On the smallness of sinking regions in the ocean. *Proc. Nat. Acad. Sci., USA*, **48**, 766–772.

Whitehead, J. A. Jr., 1980: Rotating critical flows in the ocean. *Second Int. Symp. on Stratified Flows.* Torkild Carstins and Thomas McClimans, Eds., Taper Press, Trondheim, 501 pp.

——, and D. L. Porter, 1977: Axisymmetric critical withdrawal of a rotating fluid. *Dyn. Atmos. Oceans*, **2**, 1–18.

——, A. Leetmaa and R. A. Knox, 1974: Rotating hydraulics of strait and sill flows. *Geophys. Fluid Dyn.*, **6**, 101–125.